18. Infra-Red Imaging Subsystem (IRIS)

Instrument Parameters

Brodsky (1991) suggests the following parameters for remote sensing instruments:

- focal plane detector, pattern, and cooling
- dwell time on each IFOV
- aperture size
- focal length of the collection subsystem
- instantaneous field of view (IFOV, which implies a particular ground resolution for a given orbital altitude)
- scanning scheme and swath size
- stability and figures of key electronic systems
- percentage of scene overlap
- pointing and stability requirements
- scale of images
- calibration scheme
- figures for the optical train

The stability and figures of key electronic systems, and precise figures for the optical train, are yet to be analyzed. Pointing will be based upon a nominal nadir-pointing attitude. The maximum pointing stability that can be achieved by gravity gradient and dynamic magetorquing techniques is an issue for ongoing investigation and in-flight experimentation. Pitch and roll accuracies of 0.4º have been predicted for a 250 kg spacecraft having a single gravity boom and active magnetorquing (Bryce and Raju, 1991), although a spacecraft of 50 kg mass or less is not expected to approach this stability. Instrument calibration will be against known ground targets. The remaining parameters are considered below.

Focal Plane Detector, Pattern, and Cooling

The focal plane detector used by IRIS is an EEV CCD17 device with the following characteristics:

Image Format:	512 x 512
Pixel Size:	15 μm square
Image Area:	7.7 mm x 7.7 mm
Min. readout time:	5 ms
Shuttering:	frame transfer
Exposure Control:	electronic

Output Responsivity:	2.2 μV / electron
Peak Signal:	220 mV
Dynamic Range:	> 1000:1
Binning Capacity	
in Readout Register:	x 4
Min. Array Readout Time	
- through 1 amplifier:	10 ms
- through 2 amplifiers:	5 ms
Spectral Band:	400 nm - 1100 nm
Peak Spectral Response λ:	820 nm
Quantum Efficiency:	~20%.
Phasing:	3-phase.
Illumination:	front side.

This device has been chosen due to its high resolution and dynamic range, small size and mass, and the convenience and simplicity of subsystem design when a solid state array detector is used.

Radiometric Analysis

Dwell Time vs Ground Resolution

AUSTRALIS-1 will be stabilized with a nadir-pointing z-axis with which the IRIS optical axis is aligned, so the imaging target will be the sub-satellite point on the surface of the Earth. The satellite ground velocity for the design orbital altitudes will therefore impose constraints upon the pixel ground resolution / exposure time options available. In particular, shorter exposure times will allow finer ground resolution, while longer exposure times will require coarser ground resolution. Here an expression will be provided for relating minimum ground resolution, R, to exposure time, T_e.

The circumference of the Earth is given by $2\pi R_e$, where R_e is the radius of the earth (6367 km).. Hence the satellite ground velocity in the direction of travel, V_g, for an altitude of 750 km and an orbital period of 100 minutes is given by:

$$V_g = 2\pi R_e / P = 6.67 \text{ km s}^{-1}$$

It follows from Shannon's sampling theorem (see Van Den Enden and Verhoeckx, 1989) that the imaging array can only detect unaliased spatial frequencies of less than half those defined by the highest spatial frequency of the pixel array divided by the image scale. However, for a moving image, image smear will invalidate the result unless it is itself restricted to less than half a ground pixel during an exposure. Hence, the satellite ground speed multiplied by the exposure time, T_e, must be less than half of one ground pixel, S (in m). That is:

$$S/2 > T_e.V_g \times 10^3$$

Hence the maximum exposure time bound for a given ground resolution is given by:

$$T_e < S/(2.V_g \times 10^3)$$

$$= S / 13.34 \times 10^3 \quad (1)$$

Radiative Signal Strength

This section derives a maximum expected value for the power of reflected solar radiation reaching the spacecraft, within the design bandwidth of the IRIS detector (700 nm to 1100 nm). The 700 nm to 1100 nm spectral range has been chosen for high ground cover contrast (see, for eg., Harris, 1987, Fig. 2.6).

The Sun has an average surface temperature of about T = 5800 K, an emissivity ε = 0.99, radius $R_s = 6.96 \times 10^8$ m, and distance $D = 1.496 \times 10^{11}$ m from the Earth. Treating the Sun as a black-body radiator, total emitted solar power , or exitance, is (Rees, 1990):

$$Q_{sun} = 4\pi R_s^2 T^4 \sigma\varepsilon$$

$$= 3.87 \times 10^{26} \text{ W}.$$

where σ is the Stefan-Boltzmann constant (5.67×10^{-8} Wm^{-2} K^{-4}). Irradiance at the top of the atmosphere of the Earth, E_e, is given by:

$$E_e = Q_{sun}/4\pi D^2$$

$$= 1.376 \times 10^3 \text{ Wm}^{-2}.$$

The amount of solar exitance emitted in the wavelength range from 700 nm to 1100 nm can be found by integrating the black-body radiation curve between those limits. Since the integration is difficult, Rees Table 2.2 can be used to obtain normalised (ie. proportional) values. Then:

$$E_e = 377.4 \text{ Wm}^{-2}.$$

The reflectivity, or albedo, r, of a surface expresses the ratio of total power scattered from the surface to the total incident power as a function of incidence direction. Diffuse, or hemispherical, albedo, r_d, expresses the average reflectivity with isotropic incident power. The amount of solar radiation reflected from the Earth towards the spacecraft can be modelled as a function of the albedo of the Earth 's surface, the roughness of the surface, the angle of incidence, and the reflectance angle (ie. look angle of the spacecraft, referenced to the normal to the Earth's surface at the target ground point). To determine a maximum signal strength, incidence and reflectance angles of zero will be assumed. It is further assumed that most objects of interest will be closer to Lambertian scatterers, rather than specular scatterers. Most objects have a reflectance in the range 0.3 - 0.7, so 0.7 will be taken as a design maximum (only snow is expected to exceed $r_d = 0.7$ in the 700 nm to 1100 nm band; see Rees, 1990, Fig 3.7). Hence, the reflected solar

radiation power, or Earth radiant exitance, in the spectral range from 700 to 1100 nanometers is given by:

$$M_e = E_e \cdot r_d$$

$$= 264.2 \text{ Wm}^{-2}$$

Earth's radiance is given by (Rees, 1990):

$$L = M_e / \pi$$

$$= 84.0 \text{ Wm}^{-2} \text{ sr}^{-1}.$$

Total atmospheric attenuation in the spectral band from 700 nm to 1100 nm is a factor of about 0.64, so, taking a double traversal through the atmosphere into account, the radiance is further reduced by a factor of about 0.4, resulting in L = 34.3 Wm^{-2} sr^{-1}.

Detected Radiance

The CCD detector has a peak charge storage of 10^5 electrons. The energy absorbed by each electron is given by $h\nu$, where h is Planck's constant (= 6.626×10^{-34} J.s^{-1}) and ν is the average frequency, given by $\nu = 2 \cdot c / (750 \text{ nm} + 1100 \text{ nm}) = 3.243 \times 10^{14}$ Hz (where c is the speeed of light). For detector saturation, the total energy absorbed is:

$$E = 10^5 \text{ electrons} \times h\nu$$

$$= 2.15 \times 10^{-14} \text{ J.}$$

Detected radiance is a function of radiative signal strength, optical aperture radius (R_a), orbital height, losses in the optical chain, detector quantum efficiency (Q), integration time, and losses and noise in the electronic signal acquisition and conditioning chain. Losses and noise in the optical chain and electronics can be approximated by a factor K = 0.7, to give total losses of 30%. Detector quantum efficiency, Q, is about 0.2, or 20%. Earth's effective radiance in the 700 - 1100 nm band is L = 34.3 Wm^{-2} sr^{-1} (see above). The power collected by a lens subsystem is given by the radiance of the object multiplied by the area of the object, multiplied by the solid angle of the lens into which the object radiates (Welford, 1988). For a square ground pixel, the area is S^2 (in units of m^2) the radiance is L = 34.3 Wm^{-2} sr^{-1}, and the solid angle radiated into is determined by the instrument aperture radius, R_a, and the distance to the object, h. Hence, the energy received at the detector, E_{rec}, during an exposure of duration T_e, at an altitude of 750 km, is given by:

$$E_{rec} = Q \cdot K \cdot L \cdot \pi \cdot \text{atan}^2(R_a / 750 \text{ km}) \cdot T_e \cdot S^2 \qquad (2)$$

The limiting value of atan θ as θ tends to zero is θ, so for small values of R_a / h, R_a / h can be used instead of atan(R_a / h). So, for saturation of the detector,

$$2.15 \times 10^{-14} = Q \cdot K \cdot L \cdot \pi \cdot (R_a / 750 \text{ km})^2 \cdot T_e \cdot S^2$$

That is:

$$1.42 \times 10^{-15} = (R_a / 750\ km)^2 . T_e . S^2 \quad (3)$$

A suitable subsystem design is one which involves choices for optical aperture radius, ground pixel size, and exposure time, that satisfy equation (3). Such a design will fully utilise the dynamic range of the detector.

Taking equation (1) as an equivalence, substituting into (3), and rearranging, the minimum ground resolution limit is given by:

$$S = 2.2 R_a^{-2/3} \quad (4)$$

where S and R_a are in metres. Given an aperture radius, R_a, equation (4) can be used to specify the best possible ground resolution for the subsystem for an orbital altitude of 750 km, as limited by the subsystem radiometric characteristics.

IRIS Optical Specification

The IRIS optical subsystem design is constrained by overall size and mass limitations of the AUSTRALIS-1 spacecraft. In particular, the instrument must fit within the 350 mm cube of the spacecraft while leaving sufficient room for other subsystems. The optical window in the -z face of the spacecraft reduces the number of solar cells on that face. An optimal use of the surface suggests that the optical window should be slightly less than (eg. 10 mm less than) an integer multiple of the solar cell dimensions. Each cell measures 68 mm x 68 mm, with an allowance of a further 2mm per cell for intercell gaps. Hence, 70 x n - 10 mm optical apertures can be evaluated for a suitable range of values of n. Since the spacecraft must accommodate other subsystems in addition to the imaging payload, the evaluation will be limited to 60 mm, 130 mm, and 200 mm apertures. Performance at the average design orbital altitude of 750 km will be considered.

Signal-power-limited values of S obtained by the application of Equation (4) are shown on Table 1. Assuming perfect optics, the resolution limit of a telescope due to the optical point spread function, ie. the diffraction limit β_{min}, is defined by (Welford, 1988):

$$\beta_{min} = 0.61 \lambda / R_a \quad (5)$$

where λ is the longest wavelength of incident light (1100 nm) for the spectral band of interest, and R_a is the radius of the optical aperture. Diffraction-limited performance figures obtained by applying Equation (5) are shown on Table 1. Comparison of the tables shows that subsystem performance is marginally signal-power-limited.

It is also necessary to determine the focal length of the lens and its diffraction-limited resolution. The focal length is given by:

$$f = r_d h / S \quad (6)$$

where h is the orbital altitude, S is the ground resolution of a pixel, and r_d is the length of a pixel in the image plane, that is, 15×10^{-6} m.

Table 1. Subsystem performance figures.

Aperture radius, Ra (m)	Pixel size, S at 750 km (m)	Ground diffraction circle diameter (m)	Swath at 750 km (km)	Instrument FOV (^{o})	focal length, f (m)	Maximum exposure time (ms)
0.03	22.8	16.8	11.6	0.9	0.5	1.71
0.065	13.6	7.74	7.0	0.5	0.8	1.02
0.10	10.2	5.03	5.2	0.4	1.1	0.76

The instrument field of view (FOV) limits the telescope type that can be used. Cassegrain telescopes can achieve an FOV of 0.2^o, whereas Ritchey Chretien designs can achieve up to 0.8^o. A refracting design can achieve up to 100^o, making it appropriate for the IRIS subsystem. Examination of Table 1 indicates that, due to the comparatively long focal lengths, a compound optical design would be required to achieve the stated resolutions. While aperture values up to 200 mm have been considered here, this is very large in relation to the overall size of this spacecraft (nominally, a 350 mm cube). The optical bench, shuttering, and thermal subsystem would take additional volume and mass. Overall, it is likely that a 60 mm diameter aperture is most suitable. However, the values obtained reflect the best possible performance using the EEV CCD17 array detector. In practice, the qualitiy of optics required to achieve the values obtained are likely to prohibitive, so further tradeoff studies will be required. Finally, the stated instrument field of view is considerably less than the stabilisation accuracy expected using gravity gradient and active magnetorquing methods.

Optical Filtering

Filtering is required since the CCD detector sensitivity ranges from 400 nm to 1100 nm. Band rejection filtering will be used to attenuate the band from 400 nm to 700 nm to reduce scattered light detection and to ensure good contrast between types of ground cover. The narrow FOV suggests a choice between bulk absorption filters and interference filters (Peace, 1991).

Sampling theory also shows that aliasing of spatial frequencies greater than the Nyquist frequency will occur at the image plane unless steps are taken to filter the spatial bandwidth of the instrument. The Nyquist frequency is equivalent to half the spatial frequency of CCD pixels in the image plane (with equivalent frequencies along each orthogonal axis of the plane in this case). Appropriate low pass filtering is achieved by blurring the image (Peace, 1991), already effectively accomplished in the present case since the telescope diffraction limit is close to the detector FOV (ie. 15 µm by 15 µm).

Image Plane Focus

IRIS Control Registers

The following camera control signals will be supported:

camera_on	- initiates camera unit power on / off
exposure_count	- the number of exposure clock cycles to count in order to time exposure duration
row_start_offset	
row_stop_offset	
column_start_offset	
column_stop_offset	- subframe sampling definition. Only the array area coresponding to row and column pixel counts between these offsets will be output.
row_binning_code	- two bit signal indicating on-chip binning of up to four pixels from adjacent rows
col_binning_code	- two bit signal indicating on-chip binning of up to four pixels from adjacent columns
exposure_trigger	- signal to initial electronic shutter opening (corresponding on the CCD chip to a complete frame transfer, with no output)
CDS_on	- turns correlated double sampling (CDS) on / off (CDS means that the reset output value, or averaged value, is measured before each pixel value, and the data value taken to be the difference between the two)

focal length ??? (esp. to accommodate orbital height varns.)

IRIS Controlled State Transitions

The *IRIS imaging subsystem* has four primary states, each associated with a pair of output signals, as shown on Figure ?. The *standby* state (¬DR, ¬RD) is a low-power quiescent state during which no camera operations are carried out. The *input parameters* state (¬DR, RD) will initiate the transfer of image parameters for the next image acquisition operation from the Image Request Database (IRDB). The *acquire image* state (DR, RD) is the state in which the camera actually acquires an image. The *send data* state (DR, ¬RD) is the state in which an acquired image is transferred with its associated header information to the Image Store Database. The arcs on Figure ? are labelled with the actuator signals that must be asserted by the control subsystem in order to initiate the state transition. Output values associated with each respective state are only asserted when the operation associated with the state has been completed.

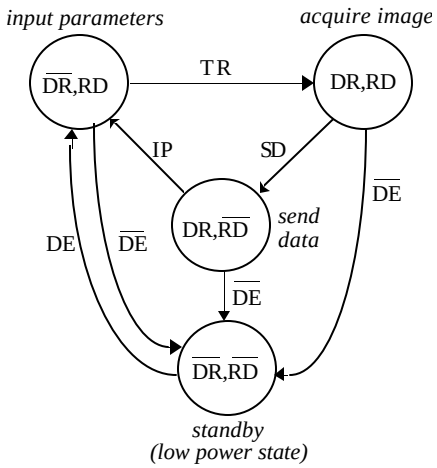

Figure ??. State transition diagram for the IRIS camera subsystem.

IRIS Status Registers

IRIS Data Ports

IRIS Analog Sensor Outputs

Signal Processing

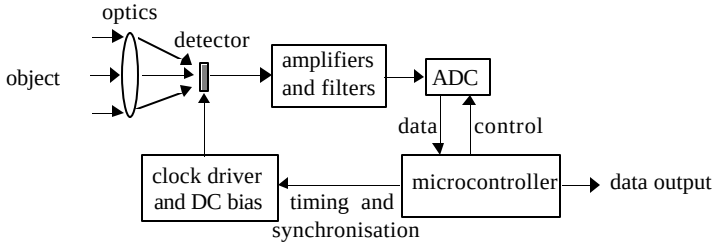

Figure ?.

Image Processing

- nonuniformities can be systemmatically eliminated by dividing the object image by a flat-field frame.

- bias value = readout value with zero exposure time. This must be subtracted (as a mean bias frame) from every image prior to any other arithmetic manipulation (McLean, 1989).

Depending upon the radiometric accuracy required in images, steps from the following sequence can be used for the reduction and calibration of raw front-side illuminated CCD images (based upon a sequence suggested by McLean, 1989):

1. subtract bias and bias structure. The bias level is a small positive voltage offset which prevents negative-going signals caused by readout noise from going into the ADC. The median of a number of bias frames can be used , a single scalar bias number can be subtracted from a single pixel, or bias values can be obtained by overscanning (see MacLean, 1989).

2. subtract the dark field

3. divide by the flat field. Pixel non-linearities tend to vary with incident light frequency

4. interpolate over bad pixels

5. remove cosmic ray events

6. registration of frames

7. median filtering

Other forms of image processing (= a user-selectable range)???

Compression strategies ???

Operating Modes

A nadir overlap (ie. spillover between adjacent detectors) is standard (Brodsky, 1991). This amounts to a time between initiation of successive exposures of ??? (need figs. for both 500 and 1000 km??). - sets frame rate for continuous coverage

- frame rate for stereogrammatic images?